Response to Anonymous Referee #2’s comments on manuscript egusphere-2022-895

We thank the reviewer for the immensely helpful comments. In response, we have carefully addressed the referee's concerns with this work. Please see point-by-point response to the comments and the revised manuscript for details. The reviewer’s comments are shown in black *italics*. Our replies are shown in indented black text.

The manuscript investigates the sensitivity of simulated $PM_{2.5}$ *and its components’ concentrations to the uncertainties in the component-specified* $PM_{2.5}$ *source emission inventories using the CMAQ chemical transport model. The relatively-complete chemical components, including Al, Ca, Cl, EC, Fe, K, Mg, Mn, Na, OC Si,* NH_4^+, NO_3^-, SO_4^{2-}, *and others, are taken into account in the emission inventory used. The authors showed that the influence of the relative contributions of different components to the total* $PM_{2.5}$ *emission (denoted as source profile changes in the manuscript) on simulated* $PM_{2.5}$ *concentration was insignificant, but its impact on* $PM_{2.5}$ *components could not be ignored. They also showed that these source profile changes caused the variations in simulated gaseous pollutants’ concentrations. While such kind of model experiment should be a welcome addition to the literature on air quality model simulation, I do have concerns that the data and methodology used in this study would be* *sensible (or well introduced) and the conclusions applicable to the simulations done by other chemical transport models with different chemical and physical modules. Therefore, I cannot recommend publication the current version of this manuscript in GMD.*

The major issues are follows:

1. What is the grid resolution of the MEIC emission inventory that was used for the model simulation in this study? Is the resolution sufficiently fine for the Dom3 (4 km× 4km) simulation? What does the area marked in green in Fig. 1 refer to? No information on the regional distributions of either $PM_{2.5}$ *emission sources or their simulated concentrations is provided in the manuscript. Are all the 10 monitoring sites located in the cities of Dom3? Is there any site that is located near the desert area? Were the mineral dust emissions taken into account in the simulation?*

Response:

Thank you for your reminder. More description of simulation area is placed in Fig. 1 and emission information in Fig. S2 of the revised manuscript. To address the reviewer’s comment, additional interpretation has been made.

The grid resolution of the MEIC emission inventory was 0.25° ×0.25°; We extracted the emissions from the original national emission inventory and reprocessed the emissions into 36km×36km, 12km×12km, and 4km×4km grids for Domains 1, 2, and 3, respectively. The Inventory Spatial Allocate Tool (ISAT) was used to provide grided $PM_{2.5}$ emission inventory for the simulations. Considering the purpose of this paper is to explore how much the source profile changes will affect the simulation results, the resolution of the emission inventory is enough. For different scenarios, other modeling conditions remain the same except for the component-specified $PM_{2.5}$ source emission inventories changed.

The area marked in green in Fig. 1 is Tianjin city in the third domain (Dom 3). The third domain with a horizontal resolution of 4 km×4 km mainly focuses on Tianjin region which is marked in Fig. RF1(b) as follow (In the revised manuscript, we have replaced Fig. 1 with Fig.RF1 below to make it more clearly).

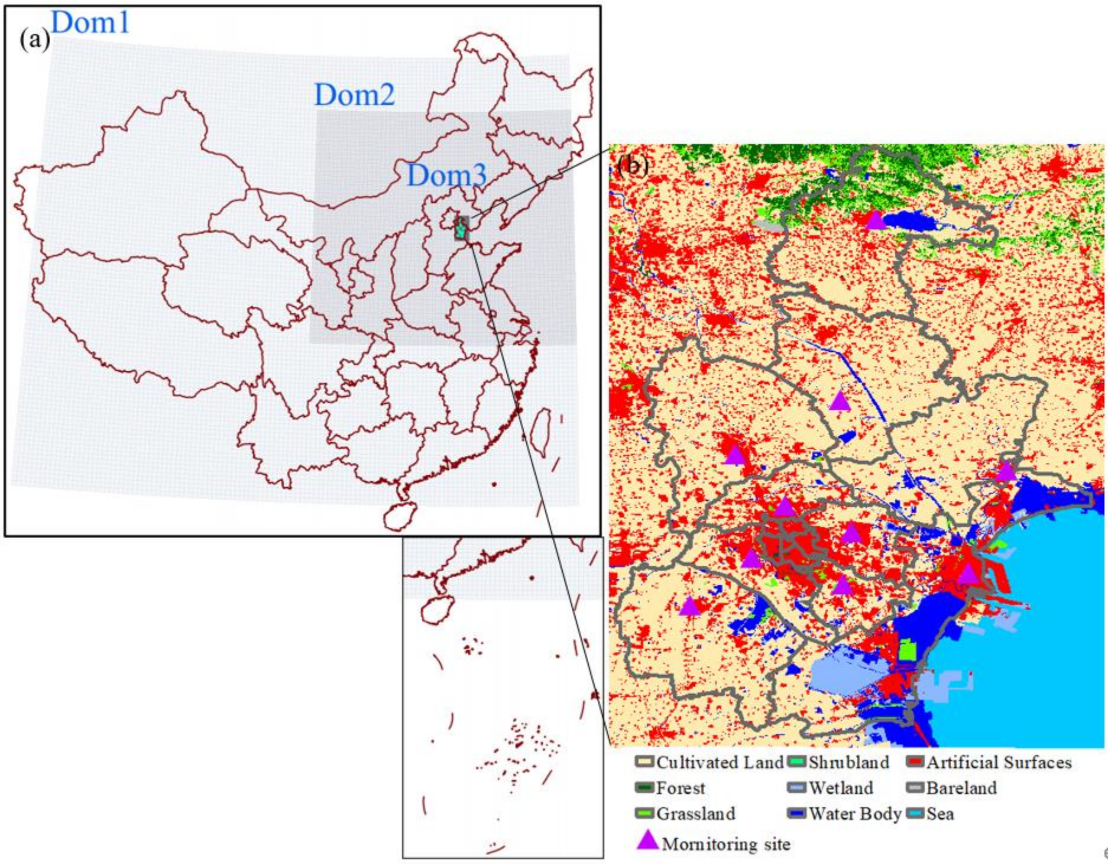

Fig. RF1 Modeling domains of the CMAQ model. (a) The three nested domains in CMAQ model; (b) Land use and observation sites of Dom3.

Data source of Land use: GLOBELAND30, www.globeland30.org, National Geomatics Center of China.

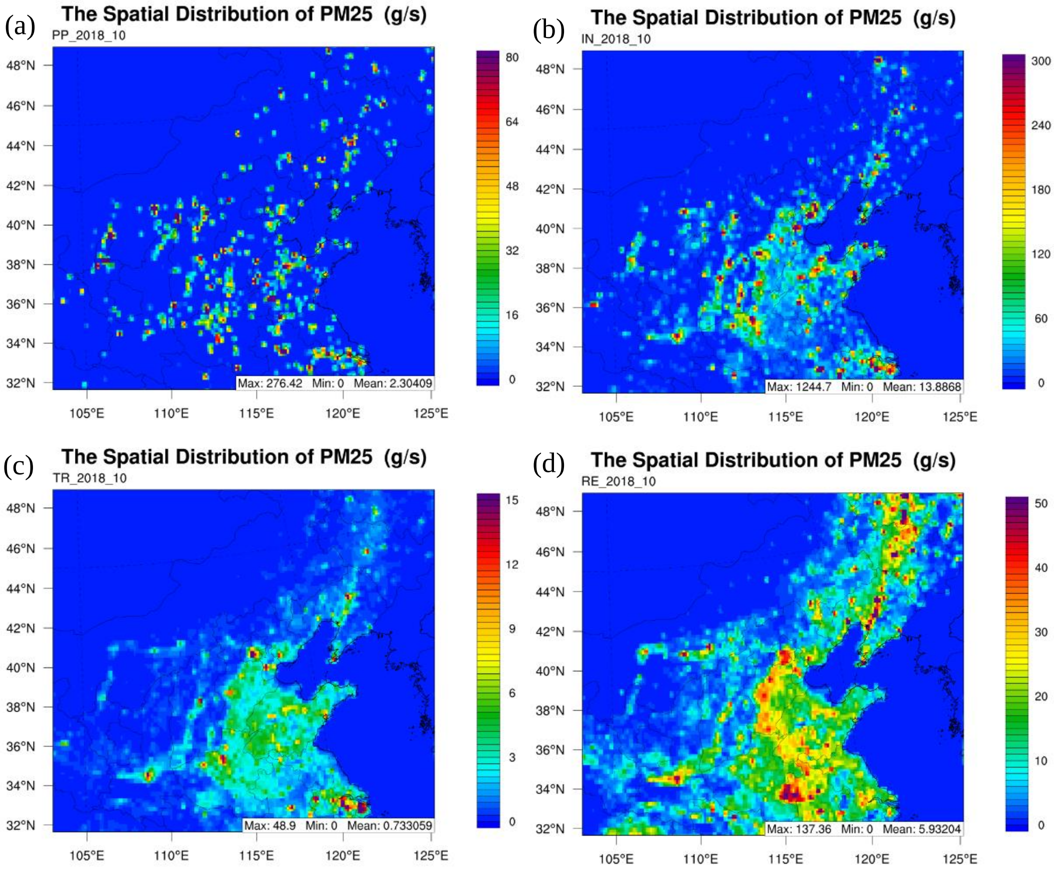

Fig. RF2 The regional distribution of $PM_{2.5}$ emission sources. (a) coal-fired power plant; (b) industry process; (c) transportation sector; (d) residential coal combustion.

The information of regional distribution of $PM_{2.5}$ emission sources are shown in Fig. RF2. In the revised manuscript, we have also provided the regional distributions of $PM_{2.5}$ emission sources (Fig. S2) in the supplementary material.

All the monitoring sites locate in the third domain which is shown in Fig. RF1(b). No sites are located in desert areas and the dust emissions are not taken into account in our simulation as the study region is far away from the deserts. The land use type of Dom3 is shown in Fig. RF1(b).

To fully address the reviewer's comment, additional interpretation has been made as follows:

In chemical transport models such as CMAQ, GEOS-Chem, CAMx, the $PM_{2.5}$ emission inventory is speciated in the chemical-composition dimension (Reff et al., 2009). Some commonly used emission inventories are listed in Table RF1. Different CTMs and their aerosol module have different regulations on $PM_{2.5}$ species types. Pollutants or species in emission inventory, especially for PM and VOCs, need to be speciated into chemical components for CTMs to match chemical mechanism. Taking CMAQ as an example, the aerosol module (AERO6) expands the definition of the PM Other species in earlier versions to include more detailed PM species (Chapel Hill, 2012); There are 18 $PM_{2.5}$ species in AERO6: OC, EC, SO_4^{2-}, NO_3^-, NH_4^+, H_2O, Na, Cl, NCOM, Al, Ca, Fe, Si, Ti, Mg, K, Mn, and Other. Other CTMs also have similar regulation, the classification of $PM_{2.5}$ species in mainstream CTMs are shown in Table RF2.

Table RF1 The air pollutants in emission inventory

Scale	Name	Air pollutants
Global	EDGAR[1]	CO, NO_x, NMVOC, CH_4; NH_3, NO_x, SO_2; PM_{10}, $PM_{2.5}$, BC, OC
Global	EDGAR-HTAP[2]	SO_2, NO_x, CO, NMVOC, PM_{10}, $PM_{2.5}$, BC, OC, NH_3
Global	GAINS[3]	SO_2, NO_X, VOC, PM, NH_3, CO_2, CH_4, N_2O and the F-gases
Reginal	MIX, MEIC[4]	SO_2, NO_x, CO, NMVOC, PM_{10}, $PM_{2.5}$, BC, OC, NH_3, and CO_2
Reginal	NEI[5]	CO, NOx, PM_{10}, $PM_{2.5}$, SO_2, VOC, NH_3
Reginal	REAS[6]	SO_2, NO_x, CO, NMVOC, PM_{10}, $PM_{2.5}$, BC, OC, NH_3, and CO_2

Reginal	EMEP[7]	SO_2, NO_x, NMVOCs, $PM_{2.5}$, NH_3

Note:

1, Emissions Database for Global Atmospheric Research (EDGAR) (1970-). https://edgar.jrc.ec.europa.eu/dataset_ap61

2, The Task Force Hemispheric Transport of Air Pollution (HTAP) (2000-2010). https://jeodpp.jrc.ec.europa.eu/ftp/jrc-opendata/EDGAR/datasets/htap_v2_2/ALL/

3, Greenhouse Gas and Air Pollution Interactions and Synergies (GAINS) (1990-).https://gains.iiasa.ac.at/gains/download/GAINS-tutorial.pdf.

4, A new Asian anthropogenic emission inventory (MIX) (2008, 2010); Multi-resolution Emission Inventory for China (MEIC) (2008-). http://meicmodel.org/

5, National emission inventory (NEI) (1970-), https://www.epa.gov/air-emissions-inventories/national-emissions-inventory-nei

6, Regional Emission inventory in Asia (REAS) (1950-2015). https://www.nies.go.jp/REAS/index.html#REASv3.2.1

7, European Monitoring and Evaluation Programme (EMEP) (1990-), https://www.eea.europa.eu/data-and-maps/dashboards/national-air-pollutant-emissions-data

Table RF2 The speciated allocation for $PM_{2.5}$ in mainstream CTMs

CTMs	Aerosol module	$PM_{2.5}$ species
CMAQ[1]	AERO6	Al, Ca, Cl, EC, Fe, K, Mg, Mn, Na, OC, Si, Ti, NH_4^+, NO_3^-, SO_4^{2-}, NCOM, Other, H_2O
	AERO5	OC, EC, NO_3^-, SO_4^{2-}, Other
GEOS-Chem[2]	aerosol.mod	Al, Ca, Cl, EC, Fe, K, Mg, Mn, Na, OC, Si, Ti, NH_4^+, NO_3^-, SO_4^{2-}, Other
WRF-Chem[3]	MADE, MOSAIC, MAM	OC, EC, NO_3^-, SO_4^{2-}, Ca, Na, Cl, H_2O, Other
CAMx[4]	CF	OC, EC, NO_3^-, SO_4^{2-}, NH_4^+, Cl, Na, Other

Note:

1, Particulate matter (aerosols): PM using three lognormal sub-distributions, or modes, two interacting modes (Aitken and accumulation) represent $PM_{2.5}$ https://www.airqualitymodeling.org/index.php/CMAQ_version_5.0_(February_2010_release)_OGD#Aerosol_Module.

2, Particulate matter in GEOS-Chem: $PM_{2.5}$ = (NH4 + NIT + SO4) * 1.10 + BCPI + BCPO + (OCPO + (OCPI * 1.05)) * (OM/OC ratio) + DST1 + DST2 * 0.30 + SALA * 1.86 + SOA * 1.05. (NIT-NO3; BCPI and BCPO-EC; OCPO and OCPI-OC, NCOM; DST1-SO4, NH4, NO3, Cl, Na, K, Ca, Fe, Al, Si, Ti, Mn, Other, OC, NCOM; DST2-SO4, Cl, ASOL; SALA-SO4, Cl, Na, Mg, K, Ca. http://wiki.seas.harvard.edu/geos-chem/index.php/GEOS-Chem_to_CMAQv5.0) http://wiki.seas.harvard.edu/geos-chem/index.php/Particulate_matter_in_GEOS-Chem.

3, Aerosols in WRF-Chem: PM using 3 or 7 log-normal modes, two interacting modes (Aitken and accumulation) represent $PM_{2.5}$.
https://ruc.noaa.gov/wrf/wrf-chem/wrf_tutorial_2018/Aerosols.pdf.
4, Aerosol Chemistry: $PM_{2.5}$ = PSO4 + PNO3 + PNH4 + PEC + NA + PCL + POA + SOA1 + SOA2 + SOA3 + SOA4 + SOPA + SOPB + FPRM + FCRS + (PFE + PMN + PK + PCA + PMG + PAL + PSI + PTI) (Fe, Mn, K, Ca, Mg, Al, Si and Ti are Optional Species).
https://camx-wp.azurewebsites.net/Files/CAMxUsersGuide_v7.20.pdf.

As total $PM_{2.5}$ need to be speciated into its chemical components to match the chemical mechanism in CTMs , emission source profiles, which can provide “species” and “split factor” for $PM_{2.5}$, are key inputs for creating chemically-resolved emission inventories for CTMs. However, the actual emission source profile of $PM_{2.5}$ and the sensitivity of simulated components’ concentrations to the variation in $PM_{2.5}$source profiles are currently not well considered. In some studies, the $PM_{2.5}$ emission inventory is speciated using “None” or “simplified profiles” in the chemical-composition dimension (Reff et al., 2009). The corresponding literature-based data is presented in Table RF3 as bellow, we only selected the main components of $PM_{2.5}$ (SO_4^{2-}, NO_3^-, NH_4^+, OC and EC) as example here. The species allocation coefficients of $PM_{2.5}$ emission sources are commonly treated in the following ways: (1) allocated $PM_{2.5}$ components of source emissions by referring to source profile data in published literature or database like the US SPECIATE; (2) chemical profiles came from local measurement. With the development of production technology and the innovation of pollution treatment technology in recent years, some source profiles have changed dramatically. The timeliness of $PM_{2.5}$ species allocation coefficients in current CTMs also need to be considered.

Although the number of $PM_{2.5}$ species and calculation method in different CTMs are different, no matter what kinds of CTMs, as long as it involves chemical components simulation for $PM_{2.5}$, the influence of source emission profiles should be considered. It remains unclear **whether the variations of adopted emission source profiles of $PM_{2.5}$ had influence on the CTMs' performance and how much the influence would be and how it works**. The purpose of this paper is to explore how much the $PM_{2.5}$ emission source profile changes will affect the simulation results. Taking CMAQ (one of the most widely used CTMs) and MEIC (a high-resolution inventory of anthropogenic air pollutants in China) as the carrier, we tested the sensitivity of the simulated chemical components to the variation of source profiles. The same kind of experiment is also applicable to other CTMs and emission inventories (e.g. NEI, EEI, REAS, HATP, etc.).

Table RF3 The adopted source profile and simulation result for different CTMs from published literatures

The component proportion in source profile	$PM_{2.5}$ components	Model	NMB	R	Study area	Period	Reference
9%	SO_4^{2-}	CMAQv4.7.1	-45%	0.73	Eastern China	2010	(Cheng et al., 2015)
1%	NO_3^-		29%	0.82			
Not explicitly Specified	SO_4^{2-}	CMAQv4.7.1	-4.5%	0.87	Qing Dao	Jan. 2016	(Zhang et al., 2017)
	NO_3^-		10%	0.87			
	NH_4^+		-6%	0.9			
Not explicitly Specified	SO_4^{2-}	CMAQv5.0.1	-54%	0.6	Northern China	2013	(Zheng et al., 2015)
	NO_3^-		-40%	0.8			
	NH_4^+		-58%	0.7			
	OC		-25%	0.8			
	EC		196%	0.6			
	SO_4^{2-}	Revised CMAQ	6%	0.7			
	NO_3^-		6%	0.8			
	NH_4^+		-4%	0.8			
	OC		-28%	0.7			
	EC		183%	0.6			
Not explicitly Specified	SO_4^{2-}	WRF-Chem3.6.1	-84%	0.31	Nanjing	Jan. 2017	(Sha et al., 2019)
			-71%	0.26		Apr. 2017	
	NO_3^-		45%	0.51		Jan. 2017	
			67%	0.32		Apr. 2017	
	NH_4^+		-34%	0.27		Jan. 2017	
			-13%	0.31		Apr. 2017	

Not explicitly Specified	SO_4^{2-}	CMAQv5.0.2	-41%	0.82	Qing Dao	Dec. 2015 ~ Jan. 2016	(Gao et al., 2020)
	NO_3^-		41%	0.83			
	NH_4^+		-5%	0.83			
Not explicitly Specified	SO_4^{2-}	RAQMS	-4%	0.83	Beijing	Feb. to Mar. 2014	(Li et al., 2020)
	NO_3^-		-4%	0.77			
	NH_4^+		4%	0.81			
	OC		-39%	0.92			
	EC		-9%	0.81			
Not explicitly Specified	SO_4^{2-}	CMAQv5.0.1	-56%~-29%	-	China	2013	(Shi et al., 2017)
	NO_3^-		-47%~19%				
	NH_4^+		-44%~1				
Not explicitly Specified	SO_4^{2-}	CMAQv4.7	-16% and -6%	-	USA	Jan. 2006	(Foley et al., 2010)
			-19%~-0.2%			Aug. 2006	
	NO_3^-		-5% and 1%			Jan. 2006	
	NH_4^+		13% and 14%			Jan. 2006	
			15% and -6%			Aug. 2006	
	OC		-20%			Jan. 2006	
			-49%			Aug. 2006	
	EC		-25%			Jan. 2006	
			-32%			Aug. 2006	
9%	SO_4^{2-}	CMAQv4.5.1	-34%~7%	-	USA	Jan. 2002	(Liu et al., 2010)
			-18%~-37%			Jul. 2002	
1%	NO_3^-		16%~118%			Jan. 2002	
			-69%~88%			Jul. 2002	
0%	NH_4^+		-0.5%~61%			Jan. 2002	

			-43%~53%			Jul. 2002	
30%	OC		-4%~13%			Jan. 2002	
			-71%~-64%			Jul. 2002	
24%	EC		-16%~18%			Jan. 2002	
			-39%~38%			Jul. 2002	
9%	SO_4^{2-}	CMAQv4.5.1	5%	0.7	South Eastern USA	Jan. 2002	(Zhang et al., 2013)
		CAMx-4.4.2	33%	0.6			
		CMAQv4.5.1	-39%	0.5		Jul. 2002	
		CAMx-4.4.2	-9%	0.6			
1%	NO_3^-	CMAQv4.5.1	46%	0.8		Jan. 2002	
		CAMx-4.4.2	-21%	0.8			
		CMAQv4.5.1	-62%	0.2		Jul. 2002	
		CAMx-4.4.2	-80%	0.2			
0%	NH_4^+	CMAQv4.5.1	-7%	0.8		Jan. 2002	
		CAMx-4.4.2	-8%	0.7			
		CMAQv4.5.1	-52%	0.7		Jul. 2002	
		CAMx-4.4.2	-45%	0.7			
30%	OC	CMAQv4.5.1	-15%	0.8		Jan. 2002	
		CAMx-4.4.2	-18%	0.8			
		CMAQv4.5.1	-73%	0.7		Jul. 2002	
		CAMx-4.4.2	-47%	0.7			
24%	EC	CMAQv4.5.1	-9%	0.7		Jan. 2002	
		CAMx-4.4.2	5%	0.7			
		CMAQv4.5.1	-47%	0.4		Jul. 2002	
		CAMx-4.4.2	-33%	0.4			

9%	SO_4^{2-}	CMAQv5.0	0.7% and -31%	0.85	USA	1990-2010	(Xing et al., 2015)
			-2%	0.61	Europe		
1%	NO_3^-		56%~59%	0.66	USA		
			-6%	0.70	Europe		
0%	NH_4^+		-13%	0.52	USA		
			34%	0.62	Europe		
Not explicitly Specified	SO_4^{2-}	CMAQv4.5	-16%	0.82	USA	2002~2008	(Friberg et al., 2016)
	NO_3^-		72%	0.64			
	NH_4^+		13%	0.68			
	OC		-30%	0.39			
	EC		-22%	0.5			
Not explicitly Specified	SO_4^{2-}	CMAQv5.0.2	-50%~29%	-	California	2013	(Chen et al., 2020)
	NO_3^-		-27%~48%				
	NH_4^+		-32%~130%				
	OC		-35%~13%				
	EC		0~43%				
The emission inventories for SO_4^{2-}, NO_3^- and NH_4^+ emitted from residential coal combustion were established	SO_4^{2-}	GEOS-Chem v11-01	Quite different		China	2015	(Yan et al., 2020)
	NO_3^-						
	NH_4^+						
Not explicitly Specified	SO_4^{2-}	WRF-Chem	MB=5μg/m^3	RMSE=12.5μg/m^3	BTH, China	2014	(Li et al., 2018)
	NO_3^-		MB=-0.3μg/m^3	RMSE=14.3μg/m^3			

	NH_4^+		MB=-0.4μg/m^3	RMSE=8.2μg/m^3			
Local source profile	SO_4^{2-}	CAMx		0.32	Tianjin	2017-2018	(Ma et al., 2022)
	NO_3^-			0.59			
	OC			0.27			
	EC			0.47			

2. At the beginning of Sect. 2.2 it is stated that in addition to SPA and SPE, the $PM_{2.5}$ *emission source profile database from published literature was used. Where and what are the final, merged emission source profiles used in this study? The simulated* $PM_{2.5}$ *and its components' concentrations using CMAQ_SPA are compared with those using CMAQ_SPE. However, no comparison with observed* $PM_{2.5}$ *components' concentrations at the monitoring sites has been made to show the advantage of the SPA over the SPE.*

Response:

More descriptions of source profiles are shown in Fig. S1 and Table S26 of our revised supplementary material. In addition, to address the reviewer's comment, we added an extra explanation as follows:

In this study, for SPE, the selected source profile of each source category group was the average/median profile developed from original profiles in SPECIATE database. The source profile codes for power plant (PP), industrial process (IN), residential coal combustion (RE), and transportation sector (TR) are 900162.5, 91155, 91022 and 91162, respectively. Please see Table RF4 for details. For SPA, the selected source profiles were from database of Source Profiles of Air Pollution, they are also available in our previous paper (Bi et al., 2019). The detailed information of source profiles as shown in the following Fig. RF3 and

Table RF4. They have also been updated in the revised supplementary material (Fig. S1 and Table S26).

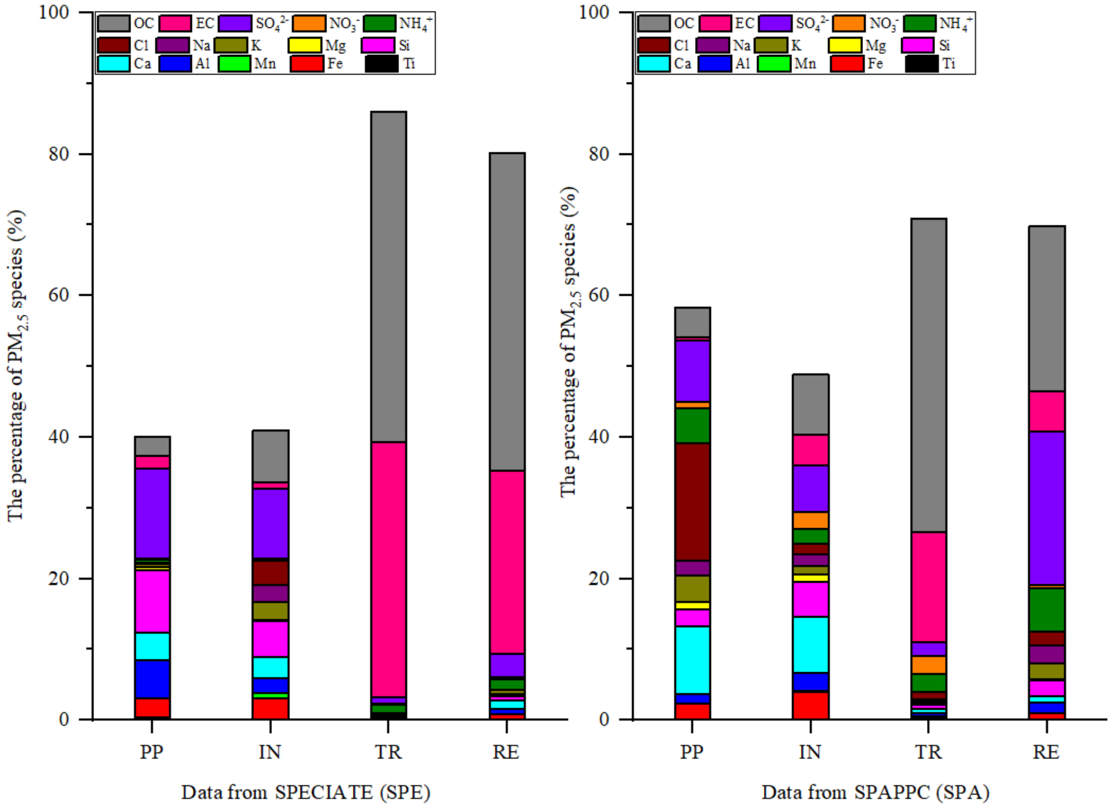

Fig. RF3 The selected speciation profile of $PM_{2.5}$ for case CMAQ_SPE and CMAQ_SPA

In SPE, the selected source profiles were average profile developed from original profiles of the source category group in SPECIATE database, the power plant (PP) source profile code was 91041, industrial process (IN) was 900162.5, Residential coal combustion (RE) was 91155, Transportation sector (TR) was 91022 and 91162. In SPA, the selected source profiles were from SPAPPC database which were measured from local emission sources.

Table RF4 The selected information of source profile in SPECIATE and SPAPPC database

Code	Profile Name	Controls	Profile Date	Profile Notes	Keywords
91041[a]	Draft Sub-Bituminous Combustion - Composite	Mixture of Baghouse, None, Electrostatic Precipitator, Wet Scrubber, Mechanical Collectors, Dry Lime Scrubber,	2006-5-24	Replaced by Profile 91110. Median of Profiles 3191, 3192, 3690, 3694, and 3700.	Sub-Bituminous Coal Combustion; PM Composite

		Ammonia Injection			
900162.5[b]	Industrial Manufacturing - Average	Not Applicable	1989-1-5	Average profile developed from original profiles representing the source category group 3xxxxxxx.	INDUSTRIAL
91155[c]	Residential Coal Combustion - Composite	Uncontrolled	2009-7-12	Median of Profiles 3761, 432012.5	Residential Coal Combustion; Inventory speciation
91022[a]	Draft On-road Gasoline Exhaust - Composite	Mixture of Catalytic converter and Not available	2006-5-24	Replaced by Profile 91122. Median of Profiles 311072.5, 3517, 3884, 3892, 3904, 3947, 3951, 3955, 3959, and 4558.	On-road Gasoline Exhaust; PM Composite
91162[c]	LDDV Exhaust - Composite	Mixture of Catalytic converter and Not available	2009-7-12	Median of Profiles 321042.5, 3912, 3963, 4675	LDDV Exhaust; Inventory speciation
Local	PP	Mixture of Baghouse, None, Electrostatic Precipitator, Wet Scrubber, Mechanical Collectors, Dry Lime Scrubber,		Average of profiles power and heating power plant	

Local	IN	Wet Scrubber, Dry Lime Scrubber,	Average of profiles steel, metallurgy, cement, glass, industrial boiler
Local	TR	Mixture of Catalytic converter	Average of profiles gasoline, diesel, gasoline-diesel exhaust
Local	RE		Average of profiles civil boiler

a, Hsu, Ying, Randy Strait, Stephen Roe, David Holoman. 2006. 'SPECIATE 4.0 Speciation database development document - Final Report', Prepared for US EPA, RTP, NC, EPA Contract Nos. EP-D-06-001, Work Assignment Numbers 0-03 and 68-D-02-063, WA 4-04 and WA 5-05, by E.H. Pechan & Associates, Incorporation, Durham, NC. https://www.epa.gov/sites/production/files/2015-10/documents/speciatedoc_1206.pdf.

b, Shareef, G. S. Engineering Judgement, Radian Corporation. August 1987.

c, Reff, Adam, Prakash V Bhave, Heather Simon, Thompson G Pace, George A Pouliot, J David Mobley, and Marc Houyoux. 2009. 'Emissions Inventory of $PM_{2.5}$ Trace Elements across the United States', Environmental Science & Technology, 43, no. 15: 5790-96. DOI: 10.1021/es802930x.

We agree with that it’s necessary to compare with observed values as to discuss the model performance, but here we mainly tried to answer (1) Whether the variation of source profile adopted in CTMs has an impact on the simulation of $PM_{2.5}$ chemical components? (2) How much does it impact? (3) How does the impact work? so we didn’t do comparison with observed $PM_{2.5}$ components’ concentrations at the monitoring sites. By comparing SPA and SPE source profiles, our purpose is to show that the source profile of same source category can vary greatly. Different simulation scenarios were designed and the sensitivity of components simulation results to $PM_{2.5}$ sources profile was explored through with chemical components of source profiles perturbation. We found that the sensitivity of simulation results to source profile changes should be considered in numerical simulation. In fact, the emission inventory, and the selection of simulated area here only are the carrier to conduct this study. Any two different groups of source profiles could be used for designing comparative experiments.

Thanks for the reviewer's valued reminder. There are several factors will influence model performance like the emission, model mechanism, meteorological modeling performance. By providing accurate and time-sensitive source profile to make the model inputs more accurate and the interference from sources on the uncertainty of simulation results is eliminated somehow. In the next work, we will use different source profile for simulation and compare the simulation results with local measured $PM_{2.5}$ components.

3. While the MEIC inventory includes four categories, i.e. power plants (PP), industrial processes (IN), residential emission (RE) and transport sector (TR), the SPA and SPE are shown to have different categories (perhaps more than the MEIC does). How were these chemical $PM_{2.5}$ *emission source profiles combined to match the MEIC categories? For instance, the residential emission should include not only coal burning but* *also straw burning, and the latter was seemly not considered in the simulations. Also, the chemical profiles for gasoline and diesel oil in the transport sector might be different.*

Response:

Thank you for your valued advices. More descriptions have been added in Section 6 (Lines 557-560 in the revised manuscript).

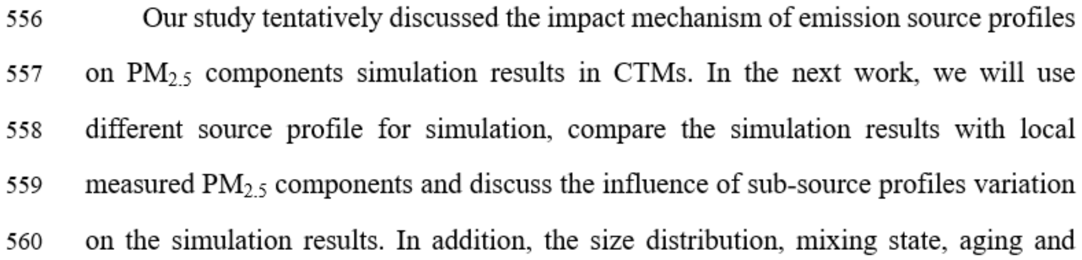

Our study tentatively discussed the impact mechanism of emission source profiles on $PM_{2.5}$ components simulation results in CTMs. In the next work, we will use different source profile for simulation, compare the simulation results with local measured $PM_{2.5}$ components and discuss the influence of sub-source profiles variation on the simulation results. In addition, the size distribution, mixing state, aging and

Just as you mentioned, in the database of Source Profiles of Air Pollution (SPAP) and U.S. Environmental Protection Agency’s (EPA) SPECIATE database, these four source categories (coal-fired power plant, industry process, transportation sector and residential coal combustion) contain a series of sub-categories. But unfortunately, the MEIC inventory does not include the corresponding sub-categories. So we take the average values of all source profiles in each source category as representing source profile, the details could be seen in our previous work (Bi et al., 2019); Then multiply inventory emissions by profile fraction to get emissions of specific chemical compounds. The general step for speciation is shown in Fig. RF4.

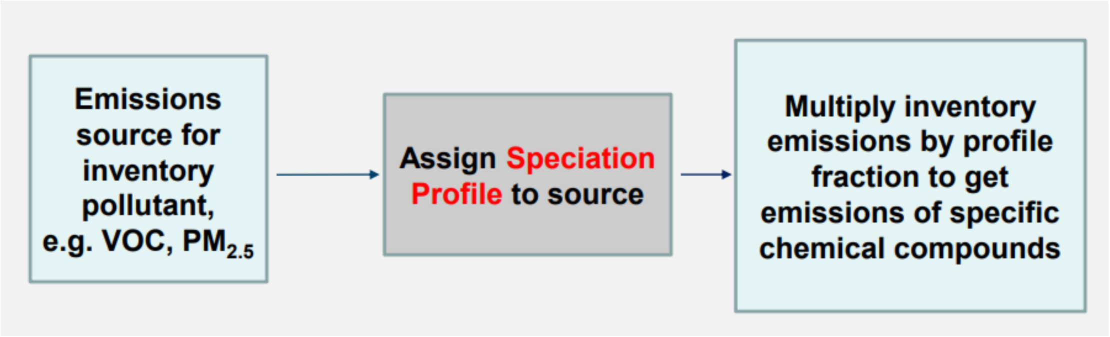

Fig. RF4 Speciation in general step

Source: International Emissions Inventory Conference. SPECIATE and using the Speciation Tool to prepare VOC and PM chemical speciation profiles for air quality modeling, p31. https://www.epa.gov/sites/default/files/2017-10/documents/speciate_speciationtool_training.pdf.

In our study, we found that the simulated concentration of $PM_{2.5}$ components, not only primary components but also secondary components, indeed varied with the source profiles. The representativeness and timeliness of source profile should be considered due to the underappreciated impact of emission source profiles on the simulation of $PM_{2.5}$ components. Thank you for your valuable comments, we will deeply discuss the influence of sub-source profiles on the simulation results in the follow-up study.

4. How are the dynamic, microphysical and chemical processes of aerosols treated in the CMAQ model used for this study? Are the size distribution, mixing state, aging and solubility taken into account for different aerosol components? By which molecular form are the chemical components (Al, Ca, Cl, EC, Fe, K, Mg, Mn, Na, OC Si, NH_4^+, NO_3^-, and SO_4^{2-}) emitted from the sources? Taking elemental Ca as an example, it should be emitted *by CaO, $CaCO_3$, $CaSO_4$, or other compound, rather than merely by the cation Ca^{2+}. The similar principle applies for anions (NO_3^- and SO_4^{2-}). The difference in the exiting form of these emitted aerosol components might have large impacts on the thermodynamic equilibrium of ions in liquid aerosols and clouds.*

Response:

Thank you for the reviewer's questions, more descriptions have been added in Section 6 (Lines 560-563 in the revised manuscript).

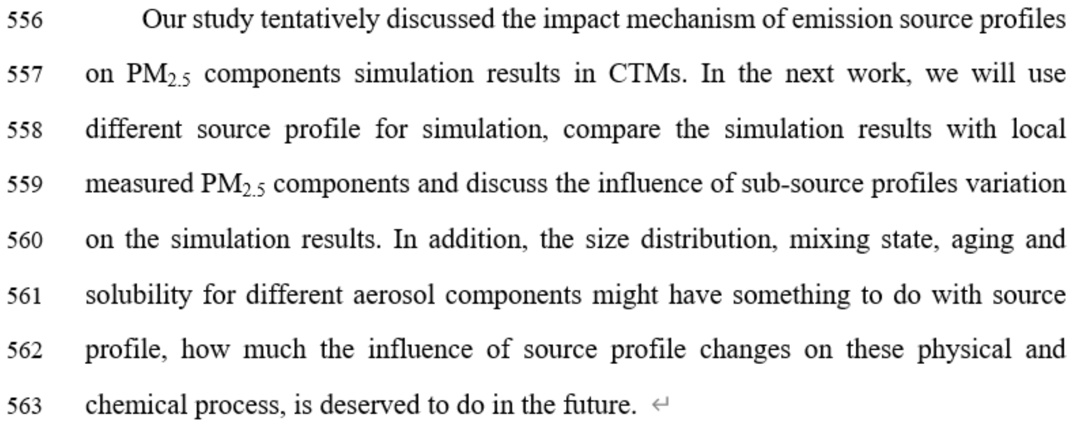

Our study tentatively discussed the impact mechanism of emission source profiles on $PM_{2.5}$ components simulation results in CTMs. In the next work, we will use different source profile for simulation, compare the simulation results with local measured $PM_{2.5}$ components and discuss the influence of sub-source profiles variation on the simulation results. In addition, the size distribution, mixing state, aging and solubility for different aerosol components might have something to do with source profile, how much the influence of source profile changes on these physical and chemical process, is deserved to do in the future.

Please see the point-by-point response as follows:

For: *How are the dynamic, microphysical and chemical processes of aerosols treated in the CMAQ model used for this study?*

The key scientific algorithms simulating aerosol processes for the CCTM in CMAQ are: (1) aerosol removal by size-dependent dry deposition; (2) aerosol-cloud droplet interaction and removal by precipitation; (3) new particle formation by binary homogeneous nucleation in a sulfuric acid/water vapor system; (4) the production of an organic aerosol component from gas-phase precursors; and (5) particle coagulation and condensation growth (Byun and Young, 1999).

The particle dynamics of aerosol distribution using three interacting lognormal distributions, or modes. Two modes (Aitken and accumulation) are generally less than 2.5μm in diameter while the coarse mode contains significant amounts of mass above 2.5μm. The equation of lognormal distribution is as follow:

$$n(\ln D) = \frac{N}{\sqrt{2\pi}\ln\sigma_g}\exp\left[-0.5\left(\frac{\ln\frac{D}{D_g}}{\ln\sigma_g}\right)^2\right] \text{……… (1)}$$

Where N is the particle number concentration within the mode suspended in a unit volume of air, D is the particle diameter, D_g is the geometric mean diameter, σ_g is the geometric standard deviation of modal distribution. A brief summary is described by (Binkowski and Roselle, 2003) and fully described by (Whitby and McMurry, 1997). The aerosol species of $PM_{2.5}$ in CMAQ are listed in Table RF5.

Table RF5 Aerosol species of $PM_{2.5}$ in CMAQ

CMAQ species	Description
AECI, AECJ	Aitken (I) and accumulation (J) mode EC mass
APOCI, APOCJ	Aitken (I) and accumulation (J) mode OC mass
APNCOMI, APNCOMJ	Aitken (I) and accumulation (J) mode primary non-carbon

	organic matter mass
ASO4J	Accumulation (J) mode sulfate mass
ANO3J	Accumulation (J) mode nitrate mass
ACLJ	Accumulation (J) mode particulate chloride mass
ANH4J	Accumulation (J) mode particulate ammonium mass
ANAJ	Accumulation (J) mode sodium mass
AKJ	Accumulation (J) mode potassium mass
AMGJ	Accumulation (J) mode magnesium mass
ACAJ	Accumulation (J) mode calcium mass
AFEJ	Accumulation (J) mode iron mass
AMNJ	Accumulation (J) mode manganese mass
AALJ	Accumulation (J) mode aluminum mass
ASIJ	Accumulation (J) mode silicon mass
ATIJ	Accumulation (J) mode titanium mass
AH2OJ	Accumulation (J) mode particulate water mass
AOTHRJ	Accumulation (J) mode remaining unspeciated fine mode primary PM mass

The aerosol microphysics i.e. coagulation, condensation, new particle formation, deposition, etc.) are considered in CMAQ using aero_subs.F, aero_depv.F, coags.f, in CCTM module correspondingly. The microphysical process and the related numerical simulation in subroutines called by the CMAQ driver are covered in more detail in the literatures (Binkowski and Roselle, 2003; Byun and Young, 1999).

The aerosol chemical species are listed in Table RF4. ISORROPIA v2.2 in the reverse mode are used to calculate the condensation/evaporation of volatile inorganic gases to/from the gas-phase concentrations of coarse particle surfaces. ISORROPIA v2.2 is also used in the forward mode to calculate instantaneous thermodynamic equilibrium between the gas and fine-particle modes. The equilibria and the associated constants are shown in Table RF6.

Table RF6 Equilibrium relations and Constants

Number	Reaction	K^0 （298.15K）
I1	$Ca(NO_3)_{2(s)} \leftrightarrow Ca^{2+}_{(aq)} + 2NO^{-}_{3(aq)}$	6.067×10^{5}
I2	$Ca(Cl)_{2(s)} \leftrightarrow Ca^{2+}_{(aq)} + 2Cl^{-}{}_{(aq)}$	7.974×10^{11}
I3	$CaSO_4\cdot 2H_2O_{(s)} \leftrightarrow Ca^{2+}_{(aq)} + SO_4^{2-}{}_{(aq)} + 2H_2O$	4.319×10^{-5}
I4	$K_2SO_{4(s)} \leftrightarrow 2K^{+}_{(aq)} + SO_4^{2-}{}_{(aq)}$	1.569×10^{-2}
I5	$KHSO_{4(s)} \leftrightarrow K^{+}_{(aq)} + HSO^{-}_{4(aq)}$	24.016
I6	$KNO_{3(s)} \leftrightarrow K^{+}_{(aq)} + NO^{-}_{3(aq)}$	0.872
I7	$KCl_{(s)} \leftrightarrow K^{+}_{(aq)} + Cl^{-}{}_{(aq)}$	8.680
I8	$MgSO_{4(s)} \leftrightarrow Mg^{2+}_{(aq)} + SO_4^{2-}{}_{(aq)}$	1.079×10^{5}
I9	$Mg(NO_3)_{2(s)} \leftrightarrow Mg^{2+}_{(aq)} + 2NO^{-}_{3(aq)}$	2.507×10^{15}
I10	$Mg(Cl)_{2(s)} \leftrightarrow Mg^{2+}_{(aq)} + 2Cl^{-}{}_{(aq)}$	9.557×10^{21}
I11	$HSO^{-}_{4(aq)} \leftrightarrow H^{+}_{(aq)} + SO_4^{2-}{}_{(aq)}$	1.015×10^{-2}
I12	$NH_{3(g)} \leftrightarrow NH_{3(aq)}$	57.64
I13	$NH_{3(aq)} + H_2O_{(aq)} \leftrightarrow NH^{+}_{4(aq)} + OH^{-}{}_{(aq)}$	1.805×10^{-5}
I14	$HNO_{3(g)} \leftrightarrow H^{+}_{(aq)} + NO^{-}_{3(aq)}$	2.511×10^{6}
I15	$HNO_{3(g)} \leftrightarrow HNO_{3(aq)}$	2.1×10^{5}
I16	$HCl_{(g)} \leftrightarrow H^{+}_{(aq)} + Cl^{-}{}_{(aq)}$	1.971×10^{6}
I17	$HCl_{(g)} \leftrightarrow HCl_{(aq)}$	2.5×10^{3}
I18	$H_2O_{(aq)} \leftrightarrow H^{+}_{(aq)} + OH^{-}{}_{(aq)}$	1.010×10^{-14}
I19	$Na_2SO_{4(s)} \leftrightarrow 2Na^{+}_{(aq)} + SO_4^{2-}{}_{(aq)}$	0.4799
I20	$(NH_4)_2SO_{4(s)} \leftrightarrow 2NH^{+}_{4(aq)} + SO_4^{2-}{}_{(aq)}$	1.817

I21	$NH_4Cl_{(s)} \leftrightarrow NH_{3(g)} + HCl_{(g)}$	1.086×10^{-16}
I22	$NaNO_{3(s)} \leftrightarrow Na^{+}_{(aq)} + NO^{-}_{3(aq)}$	11.97
I23	$NaCl_{(s)} \leftrightarrow Na^{+}_{(aq)} + Cl^{-}_{(aq)}$	37.66
I24	$NaHSO_{4(s)} \leftrightarrow Na^{+}_{(aq)} + HSO^{-}_{4(aq)}$	2.413×10^{4}
I25	$NH_4NO_{3(s)} \leftrightarrow NH_{3(g)} + HNO_{3(g)}$	4.199×10^{-17}
I26	$NH_4HSO_{4(s)} \leftrightarrow NH^{+}_{4(aq)} + HSO^{-}_{4(aq)}$	1.383
I27	$(NH_4)_3H(SO_4)_{2(s)} \leftrightarrow 3NH^{+}_{4(aq)} + HSO^{-}_{4(aq)} + SO^{2-}_{4(aq)}$	29.72

Source: (Fountoukis and Nenes, 2007)

Besides that, for a higher computational efficiency, a VBS-style approach (four surrogate species with specific vapor pressures) is widely used in models; For the nonvolatile POA configuration, mass is tracked separately in terms of its carbon (OC) and non-carbon (NCOM) content. With this approach in AERO6, mass can be added to the non-carbon species to simulate the aging of POA in response to atmospheric oxidants. Details are shown in CMAQ users guide (chapter 6, https://github.com/USEPA/CMAQ/blob/main/DOCS/Users_Guide/CMAQ_UG_ch06_model_configuration_options.md#6.11_Aerosol_Dynamics) and the literature (Binkowski and Roselle, 2003).

For: *Are the size distribution, mixing state, aging and solubility taken into account for different aerosol components?*

Yes, they are all taken into account for different aerosol components. For size distribution, taking $PM_{2.5}$ as an example, except for a very small fraction of OC, EC and non-carbon organic matter are allocated in the Aitken mode, the rest are allocated in the accumulation mode. The size distribution of different $PM_{2.5}$ components are shown in Table RF7.

Table RF7 The size distribution of different $PM_{2.5}$ components

Name	Aitken (I)	Accumulation (J)	Coarse (K)
EC	0.001	0.999	0
OC	0.001	0.999	0
NCOM	0.001	0.999	0
SO_4^{2-}	0	1	0
NO_3^-	0	1	0
Cl^-	0	1	0
NH_4^+	0	1	0
Na	0	1	0
K	0	1	0
Mg	0	1	0
Ca	0	1	0
Fe	0	1	0
Mn	0	1	0
Al	0	1	0
Si	0	1	0
Ti	0	1	0
H_2O	0	1	0
Other	0	1	0

Source: AERO_EMIS.F in CCTM module

As regards as mixing state (hetchem.f in CMAQ), the empirical equations developed by Martin et al (Martin et al., 2003) are applied to determine the crystallization relative humidity (CRH) for a given mixture of sulfate, nitrate, and ammonium. Though those equations are validated only at 293K, they are applied at all ambient temperatures because insufficient data exist to estimate the temperature dependence of the CRH of mixed sulfate-nitrate-ammonium particles.

As to aerosol aging, the subroutine of poaage.F in AERO module calculates oxidative aging of POA using the following reaction (Table RF8):

Table RF8 Oxidative aging of POA

POCRm ---> PNCOM (rate constant = koheff*[OH])
    - POCRm = reduced primary organic carbon (molar concentration)
POMOC = (POC + NCOM)/POC
    - in other words: pimary OM/OC = (POC + PNCOM)/POC
PHOrat = (44/12 - POMOC)/(POMOC - 14/12)
Omoles = NCOM/(16 + PHOrat) if POMOC is between 14/12 and 44/12
Omoles = NCOM/16 for POMOC larger than 44/12
    - if OM/OC > 3.667, then POC is fully oxidized and all NCOM is oxygen
Omoles = 0 for POMOC smaller than 14/12
    - if OM/OC < 1.167, then POC is fully reduced and all NCOM is hydrogen
POCRm = POC/12 - Omoles
NOTE: POC was divided by 12 b/c we want moles of carbon atoms not moles of POC (since each carbon atom w\in the molecule is allowed to react)

For solubility, the system modeled by ISORROPIA II consists of the following potential components: Gas phase: NH_3(g), HNO_3(g), HCl(g), H_2O(g); Liquid phase: NH_4^+(aq), Na^+(aq), H^+(aq), Cl^-(aq), NO_3^-(aq), SO_4^{2-} (aq), HNO_3(aq), NH_3(aq), HCl(aq), HSO_4^-(aq), OH^-(aq), H_2O(aq), Ca^{2+}(aq), K^+(aq), Mg^{2+}(aq); Solid phase: $(NH_4)_2SO_4$(s), NH_4HSO_4(s),$(NH_4)_3H(SO_4)_2$(s), NH_4NO_3(s), NH_4Cl(s), NaCl(s), $NaNO_3$(s), $NaHSO_4$(s), Na_2SO_4(s), $CaSO_4$(s), $Ca(NO_3)_2$(s), $CaCl_2$(s), K_2SO_4(s), $KHSO_4$(s), KNO_3(s), KCl(s), $MgSO_4$(s), $Mg(NO_3)_2$(s), $MgCl_2$(s);

where the subscripts (g), (aq), (s) denote gas, aqueous and solid, respectively.

For: *By which molecular form are the chemical components (Al, Ca, Cl, EC, Fe, K, Mg, Mn, Na, OC Si,* NH_4^+, NO_3^-, *and* SO_4^{2-}*) emitted from the sources? Taking elemental Ca as an example, it should be emitted by CaO,* $CaCO_3$, $CaSO_4$, *or other compound, rather than merely by the cation* Ca^{2+}. *The similar principle applies for anions (*NO_3^- *and* SO_4^{2-}*). The difference in the exiting form of these emitted aerosol components might have large impacts on the thermodynamic equilibrium of ions in liquid aerosols and clouds.*

Generally, the PM samples emitted from the sources are collected on Teflon and quartz fiber filters and then sent for chemical component analysis. Elements analysis uses Teflon filters, common chemical analysis instruments are: inductively coupled plasma optical emission spectrometer (ICP-OES), inductively coupled plasma atomic emission spectrometer (ICP-AES), inductively coupled plasma mass spectrometer (ICP-MS) instruments and X-ray fluorescence. The total carbon (TC) mass in the samples are typically determined using thermal or thermal–optical methods. There are two widely utilized approaches to dividing OC and EC from TC, known as IMPROVE_A (from the Desert Research Institute– DRI) and NIOSH (method 5040; from the National Institute for Occupational Safety and Health – NIOSH), which are operationally defined by the time–

temperature protocols, and the OC–EC split point is determined by optical reflectance/transmittance (Ho et al., 2003; Bi et al., 2019). PM samples collected on the quartz fiber filters are normally used for the determination of water-soluble inorganic ions via different types of ion chromatography (IC) with high-capacity cation-exchange and anion-exchange columns. In addition, the molecular form of particulate matter emitted by pollution sources is difficult to measure. Hence, data form in emission source profiles are chemical components NOT chemical compounds.

The emission input files for CTMs are generated from data provided by emission inventories, only the species that are specifically defined in the chemical mechanism will be included in model inputs and outputs. PM need to be speciated into chemical components for CTMs to match chemical mechanism, and the emission source profiles can provide “species” and “split factor”（Detail is shown in Fig. RF3）. The species for $PM_{2.5}$ in mainstream CTMs are listed in Table RF2. The process of modeling speciation requires components **rather than chemical compounds.**

Thank you for your valuable comments. Our study tentatively discussed the impact mechanism of emission source profiles on $PM_{2.5}$ components simulation results in CTMs. We found the influences are connected to model chemical mechanisms since the variation of species allocations in emission sources directly affected the thermodynamic equilibrium system. We will continue exploring the influence of source profile changes on aerosol microphysical and chemical processes in a follow-up study.

Table RF2 The speciated allocation for $PM_{2.5}$ in mainstream CTMs

CTMs	Aerosol module	$PM_{2.5}$ species
CMAQ[1]	AERO6	Al, Ca, Cl, EC, Fe, K, Mg, Mn, Na, OC, Si, Ti, NH_4^+, NO_3^-, SO_4^{2-}, NCOM, Other, H_2O
	AERO5	OC, EC, NO_3^-, SO_4^{2-}, Other
GEOS-Chem[2]	aerosol.mod	Al, Ca, Cl, EC, Fe, K, Mg, Mn, Na, OC, Si, Ti, NH_4^+, NO_3^-, SO_4^{2-}, Other
WRF-Chem[3]	MADE, MOSAIC, MAM	OC, EC, NO_3^-, SO_4^{2-}, Ca, Na, Cl, H_2O, Other
CAMx[4]	CF	OC, EC, NO_3^-, SO_4^{2-}, NH_4^+, Cl, Na, Other

Note:

1, Particulate matter (aerosols): PM using three lognormal sub-distributions, or modes, two interacting modes (Aitken and accumulation) represent $PM_{2.5}$ https://www.airqualitymodeling.org/index.php/CMAQ_version_5.0_(February_2010_release)_OGD#Aerosol_Module.

2, Particulate matter in GEOS-Chem: $PM_{2.5}$ = (NH4 + NIT + SO4) * 1.10 + BCPI + BCPO + (OCPO + (OCPI * 1.05)) * (OM/OC ratio) + DST1 + DST2 * 0.30 + SALA * 1.86 + SOA * 1.05. (NIT-NO3; BCPI and BCPO-EC; OCPO and OCPI-OC, NCOM; DST1-SO4, NH4, NO3, Cl, Na, K, Ca, Fe, Al, Si, Ti, Mn, Other, OC, NCOM; DST2-SO4, Cl, ASOL; SALA-SO4, Cl, Na, Mg, K, Ca. http://wiki.seas.harvard.edu/geos-chem/index.php/GEOS-Chem_to_CMAQv5.0) http://wiki.seas.harvard.edu/geos-chem/index.php/Particulate_matter_in_GEOS-Chem.

3, Aerosols in WRF-Chem: PM using 3 or 7 log-normal modes, two interacting modes (Aitken and accumulation) represent $PM_{2.5}$. https://ruc.noaa.gov/wrf/wrf-chem/wrf_tutorial_2018/Aerosols.pdf.

4, Aerosol Chemistry: $PM_{2.5}$ = PSO4 + PNO3 + PNH4 + PEC + NA + PCL + POA + SOA1 + SOA2 + SOA3 + SOA4 + SOPA + SOPB + FPRM + FCRS + (PFE + PMN + PK + PCA + PMG + PAL + PSI + PTI) (Fe, Mn, K, Ca, Mg, Al, Si and Ti are Optional Species). https://camx-wp.azurewebsites.net/Files/CAMxUsersGuide_v7.20.pdf.

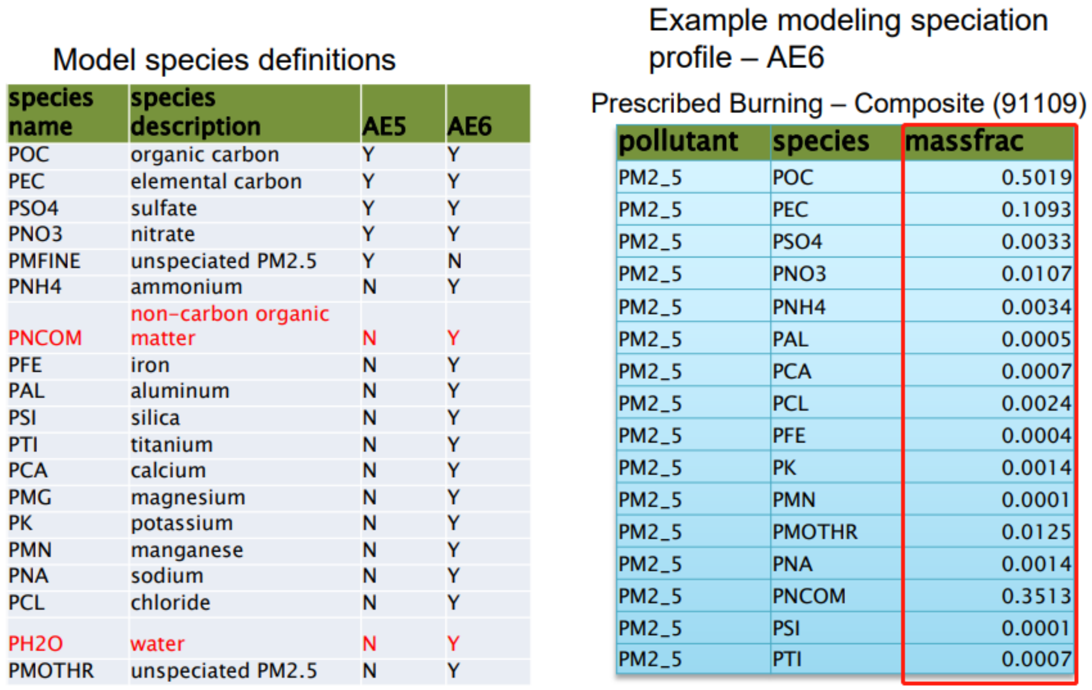

Model species definitions

species name	species description	AE5	AE6
POC	organic carbon	Y	Y
PEC	elemental carbon	Y	Y
PSO4	sulfate	Y	Y
PNO3	nitrate	Y	Y
PMFINE	unspeciated PM2.5	Y	N
PNH4	ammonium	N	Y
PNCOM	non-carbon organic matter	N	Y
PFE	iron	N	Y
PAL	aluminum	N	Y
PSI	silica	N	Y
PTI	titanium	N	Y
PCA	calcium	N	Y
PMG	magnesium	N	Y
PK	potassium	N	Y
PMN	manganese	N	Y
PNA	sodium	N	Y
PCL	chloride	N	Y
PH2O	water	N	Y
PMOTHR	unspeciated PM2.5	N	Y

Example modeling speciation profile – AE6

Prescribed Burning – Composite (91109)

pollutant	species	massfrac
PM2_5	POC	0.5019
PM2_5	PEC	0.1093
PM2_5	PSO4	0.0033
PM2_5	PNO3	0.0107
PM2_5	PNH4	0.0034
PM2_5	PAL	0.0005
PM2_5	PCA	0.0007
PM2_5	PCL	0.0024
PM2_5	PFE	0.0004
PM2_5	PK	0.0014
PM2_5	PMN	0.0001
PM2_5	PMOTHR	0.0125
PM2_5	PNA	0.0014
PM2_5	PNCOM	0.3513
PM2_5	PSI	0.0001
PM2_5	PTI	0.0007

Fig. RF3 PM$_{2.5}$ speciation- Modeling profile example

Source: International Emissions Inventory Conference. SPECIATE and using the Speciation Tool to prepare VOC and PM chemical speciation profiles for air quality modeling, p31. https://www.epa.gov/sites/default/files/2017-10/documents/speciate_speciationtool_training.pdf.

5. In Sect. 1 and Table S1, the deviations of $PM_{2.5}$ *components simulated by CMAQ are presented. All these components (*NH_4^+*,* NO_3^-*,* SO_4^{2-}*, and part of OC), except for EC and part of OC, are second aerosols, and their loadings in the atmosphere are controlled primarily by the emissions of gaseous precursors, instead of the emission of aerosols. The presentation here and associated arguments seems to be misleading as the effect of uncertainties in the gaseous emissions is not considered in this study.*

Response:

Thank you for your advices. One of the important sources of these atmospheric components (NH_4^+, NO_3^-, SO_4^{2-}, and OC) is formed by chemical conversion of gaseous precursors, which *are second aerosols*. But they still have some primary sources, a number of recent studies found that, primary emission may be also important. These components (NH_4^+, NO_3^-, SO_4^{2-}, and OC) exist in primary emission sources such as coal-fired power plant, industry process, transportation sector and residential coal combustion, the detail is shown in Fig. RF4 (Fig. 2~ 5 in manuscript); For example, sulfate (a major $PM_{2.5}$ component) is largely from primary emissions rather than secondary formation in ambient air in certain circumstances (Chen et al., 2017; Dai et al., 2019; Ding et al., 2021; Ding et al., 2019; Li et al., 2017; Yang et al., 2020; Yan et al., 2020), its weight percentage variation range is 0.7~71% in coal-fired power plant , 0.03%~40% in industry process, 0.02~40% in transportation sector, 1~40% in residential coal combustion, respectively.

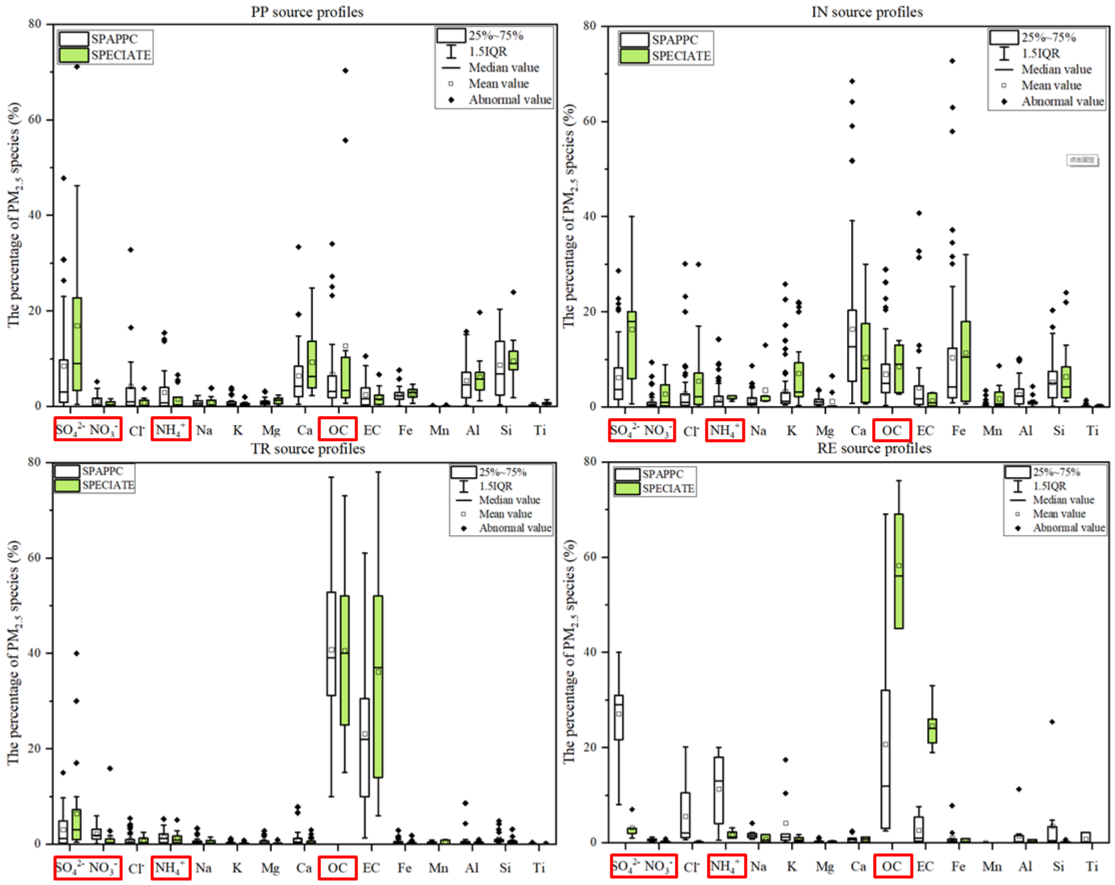

Fig. RF4 Chemical profiles for $PM_{2.5}$ emitted from coal-fired power plant (PP), industry processes (IN), transportation sector (TR), residential coal combustion (RE).

In our study, we found source profile variation could affect the simulation result of secondary components, **they could lever the whole aerosol equilibrium system.** The effects of source profile variation on the simulation results of different components were linked. When the percentages of Non-SNA, SO_4^{2-}, NO_3^- and NH_4^+ in the source profile changed, they not only affected the simulated concentration of themselves, but also affected the simulation results of some other components through the thermodynamic equilibrium system (ISORROPIA II, SO_4^{2-}-NO_3^--Cl^--NH_4^+-Na^+-K^+-Mg^{2+}-Ca^{2+}-H_2O system). Section 5 in our manuscript focused on these performances: in the sensitivity tests, when we only perturb the $PM_{2.5}$ source profile (primary emission) but not the emission inventory of gaseous precursors, the simulated result of secondary $PM_{2.5}$ components also changed, this side-fact indicates the crucial role of primary $PM_{2.5}$ components on the simulation of second components formation in CTMs.

Reference:

Bi, X., Dai, Q., Wu, J., Zhang, Q., Zhang, W., Luo, R., Cheng, Y., Zhang, J., Wang, L., Yu, Z., Zhang, Y., Tian, Y., Feng, Y.: Characteristics of the main primary source profiles of particulate matter across China from 1987 to 2017, Atmos. Chem. Phys., 19, 3223-3243, https://doi.org/10.5194/acp-19-3223-2019, 2019.

Binkowski, F., Roselle, S. J.: Models-3 Community Multiscale Air Quality (CMAQ) model aerosol component 1. Model description, Journal of Geophysical Research: Atmospheres, 108, 4183, http://doi.org/10.1029/2001JD001409, 2003.

Byun, D., Young, J.: Governing Equations and Computational Structure of the Community Multiscale Air Quality (CMAQ) Chemical Transport Model, https://www.cmascenter.org/cmaq/science_documentation/pdf/ch06.pdf

Chapel Hill, N.: Operational Guidance for the Community Multiscale Air Quality (CMAQ) Modeling System Version 5.0, https://www.airqualitymodeling.org/index.php/CMAQ_version_5.0_(February_2010_release)_OGD#Aerosol_Module, last access: February 2012.

Chen, J., Yin, D., Zhao, Z., Kaduwela, A. P., Avise, J. C., Damassa, J. A., Beyersdorf, A., Burton, S., Ferrare, R., Herman, J. R., Kim, H., Neuman, A., Nowak, J. B., Parworth, C., Scarino, A. J., Wisthaler, A., Young, D. E., Zhang, Q.: Modeling air quality in the San Joaquin valley of California during the 2013 Discover-AQ field campaign, Atmos. Environ., 5, 100067, https://doi.org/10.1016/j.aeaoa.2020.100067, 2020.

Chen, S., Xu, L., Zhang, Y., Chen, B., Wang, X., Zhang, X., Zheng, M., Chen, J., Wang, W., Sun, Y., Fu, P., Wang, Z., Li, W.: Direct observations of organic aerosols in common wintertime hazes in North China: insights into direct emissions from Chinese residential stoves, Atoms. Chem. Phys., 17, 1259-1270, https://doi.org/10.5194/acp-17-1259-2017, 2017.

Cheng, N. L., Meng, F., Wang, J. K., Chen, Y. B., Wei, X., Han, H.: Numerical simulation of the spatial distribution and deposition of $PM_{2.5}$ in East China coastal area in 2010 (In Chinese), Journ. Safety Environ., 15, 305-310, https://doi.org/10.13637/j.issn.1009-6094.2015.06.063, 2015.

Dai, Q., Bi, X., Song, W., Li, T., Liu, B., Ding, J., Xu, J., Song, C., Yang, N., Schulze, B. C., Zhang, Y., Feng, Y., Hopke, P. K.: Residential coal combustion as a source of primary sulfate in Xi'an, China, Atmos. Environ., 196, 66-76, https://doi.org/10.1016/j.atmosenv.2018.10.002, 2019.

Ding, X., Li, Q., Wu, D., Liang, Y., Xu, X., Xie, G., Wei, Y., Sun, H., Zhu, C., Fu, H., Chen, J.: Unexpectedly Increased Particle Emissions from the Steel Industry Determined by Wet/Semidry/Dry Flue Gas Desulfurization Technologies, Environ. Sci. Technol., 53, 10361-10370, https://doi.org/10.1021/acs.est.9b03081, 2019.

Ding, X., Li, Q., Wu, D., Wang, X., Li, M., Wang, T., Chen, J.: Direct observation of sulfate explosive growth in wet plumes emitted from typical coal-fired stationary sources, Geophy. Res. Lett., 48, e2020GL092071, https://doi.org/10.1029/2020GL092071, 2021.

Foley, K. M., Roselle, S. J., Appel, K. W., Bhave, P. V., Pleim, J., Otte, T., Mathur, R., Sarwar, G., Young, J. O., Gilliam, R.: Incremental testing of the community multiscale air quality (CMAQ) modeling system version 4.7, Geosci. Model Dev., 3, 205-226, https://doi.org/10.5194/gmd-3-205-2010, 2010.

Fountoukis, C., Nenes, A.: ISORROPIA II: a computationally efficient thermodynamic equilibrium model for K^+–Ca^{2+}–Mg^{2+}–NH_4^+–Na^+–SO_4^{2-}–NO_3^-–Cl^-–H_2O aerosols, Atmos. Chem. Phys., 7, 4639-4659, https://doi.org/10.5194/acp-7-4639-2007, 2007.

Friberg, M. D., Zhai, X., Holmes, H. A., Chang, H. H., Strickland, M. J., Sarnat, S. E., Tolbert, P. E., Russell, A. G., Mulholland, J. A.: Method for Fusing Observational Data and Chemical Transport Model Simulations To Estimate Spatiotemporally Resolved Ambient Air Pollution, Environ. Sci. Technol., 50, 3695-3705, https://doi.org/10.1021/acs.est.5b05134, 2016.

Gao, Y., Shan, H., Zhang, S., Sheng, L., Li, J., Zhang, J., Ma, M., Meng, H., Luo, K., Gao, H., Yao, X.: Characteristics and sources of $PM_{2.5}$ with focus on two severe pollution events in a coastal city of Qingdao, China, Chemosphere, 247, 125861, https://doi.org/10.1016/j.chemosphere.2020.125861, 2020.

Ho, K. F., Lee, S. C., Chow, J. C., Watson, J. G.: Characterization of PM_{10} and $PM_{2.5}$ source profiles for fugitive dust in Hong Kong, Atmos. Environ., 37, 1023-1032, https://doi.org/10.1016/s1352-2310(02)01028-2, 2003.

Li, J., Han, Z., Li, J., Liu, R., Wu, Y., Liang, L., Zhang, R.: The formation and evolution of secondary organic aerosol during haze events in Beijing in wintertime, Sci. Total Environ., 703, 134937, https://doi.org/10.1016/j.scitotenv.2019.134937, 2020.

Li, X., Wu, J., Elser, M., Cao, J., Feng, T., El-Haddad, I., Huang, R., Tie, X., Prevot, A. S. H., Li, G.: Contributions of residential coal combustion to the air quality in Beijing-Tianjin-Hebei (BTH), China: A case study, Atmos. Chem. Phy. Discuss., http://doi.org/10.5194/acp-2017-1237, 2018.

Li, Z., Jiang, J., Ma, Z., Fajardo, O., Deng, J., Duan, L.: Influence of flue gas desulfurization (FGD) installations on emission characteristics of PM2.5 from coal-fired power plants equipped with selective catalytic reduction (SCR), Environ. Pollut., 230, 655-662, https://doi.org/10.1016/j.envpol.2017.06.103, 2017.

Liu, X. H., Zhang, Y., Olsen, K. M., Wang, W. X., Do, B. A., Bridgers, G. M.: Responses of future air quality to emission controls over North Carolina, Part I: Model evaluation for current-year simulations, Atmos. Environ., 44, 2443-2456, https://doi.org/10.1016/j.atmosenv.2010.04.002, 2010.

Ma, S., Shao, M., Zhang, Y., Dai, Q., Wang, L., Wu, J., Tian, Y., Bi, X., Feng, Y.: Evaluating the performance of chemical transport models for $PM_{2.5}$ source apportionment: An integrated application of spectral analysis and grey incidence analysis, Sci. Total Environ., 837, 155781, https://doi.org/10.1016/j.scitotenv.2022.155781, 2022.

Martin, S., Schlenker, J., Malinowski, A., Hung, H., Rudich, Y.: Crystallization of atmospheric sulfate-nitrate-ammonium particles, Geophy. Res. Lett., 30, 2102, https://doi.org/10.1029/2003GL017930, 2003.

Reff, A., Bhave, P. V., Simon, H., Pace, T. G., Pouliot, G. A., Mobley, J. D., Houyoux, M.: Emissions Inventory of $PM_{2.5}$ Trace Elements across the United States, Environ. Sci. Technol., 43, 5790-5796, http://doi.org/10.1021/es802930x, 2009.

Sha, T., Ma, X., Jia, H., Tian, R., Chang, Y., Cao, F., Zhang, Y.: Aerosol chemical component: Simulations with WRF-Chem and comparison with observations in Nanjing, Atmos. Environ., 218, 1-14, https://doi.org/10.1016/j.atmosenv.2019.116982, 2019.

Shi, Z., Li, J., Huang, L., Wang, P., Wu, L., Ying, Q., Zhang, H., Lu, L., Liu, X., Liao, H., Hu, J.: Source apportionment of fine particulate matter in China in 2013 using a source-oriented chemical transport model, Sci. Total Environ., 601-602, 1476-1487, https://doi.org/10.1016/j.scitotenv.2017.06.019, 2017.

Whitby, E., Mcmurry, P. H.: Modal aerosol dynamics modeling, Aerosol. Sci. Technol., 27, 673-688, https://www.researchgate.net/profile/Uma-Shankar-3/publication/236373518_Modal_Aerosol_Dynamics_Modeling/links/0deec52ebc352c6bc6000000/Modal-Aerosol-Dynamics-Modeling.pdf, 1997.

Xing, J., Mathur, R., Pleim, J., Hogrefe, C., Gan, C. M., Wong, D. C., Wei, C., Gilliam, R., Pouliot, G.: Observations and modeling of air quality trends over 1990–2010 across the Northern Hemisphere: China, the United States and Europe, Atmos. Chem. Phy., 15, 2723-2747, https://doi.org/10.5194/acp-15-2723-2015, 2015.

Yan, Q., Kong, S., Yan, Y., Liu, H., Wang, W., Chen, K., Yin, Y., Zheng, H., Wu, J., Yao, L., Zeng, X., Chen, Y., Zheng, S., Wu, F., Niu, Z., Zhang, Y., Zheng, M., Zhao, D., Liu, D., Qi, S.: Emission and simulation of primary fine andsubmicron particles and water-soluble ions from domestic coal combustion in China, Atmos. Environ., 224, 117308, http://doi.org/10.1016/j.atmosenv.2020.117308, 2020.

Yang, F., Liu, H., Feng, P., Li, Z., Tan, H.: Effects of wet flue gas desulfurization and wet electrostatic precipitators on emission characteristics of particulate matter and its ionic compositions from four 300 MW level ultralow coal-fired power plants, Energ. Fuel., 34, 16423-16432, https://doi.org/10.1021/acs.energyfuels.0c03222, 2020.

Zhang, Q., Xue, D., Wang, S., Wang, L., Wang, J., Ma, Y., Liu, X.: Analysis on the evolution of $PM_{2.5}$ heavy air pollution process in Qingdao (In Chinese), China Environ. Sci., 37, 3623-3635, https://doi.org/10.3969/j.issn.1000-6923.2017.10.003, 2017.

Zhang, Y., Olsen, K. M., Wang, K.: Fine Scale Modeling of Agricultural Air Quality over the Southeastern United States Using Two Air Quality Models. Part I. Application and Evaluation, Aerosol Air Qual. Res., 13, 1231-1252, https://doi.org/10.4209/aaqr.2012.12.0346, 2013.

Zheng, B., Zhang, Q., Zhang, Y., He, K. B., Wang, K., Zheng, G. J., Duan, F. K., Ma, Y. L., Kimoto, T.: Heterogeneous chemistry: a mechanism missing in current models to explain secondary inorganic aerosol formation during the January 2013 haze episode in North China, Atmos. Chem. Phys., 15, 2031-2049, https://doi.org/10.5194/acp-15-2031-2015, 2015.